Levels of complexity in scale-invariant neural signals

Plamen Ch. Ivanov,[1,2,3,*] Qianli D. Y. Ma,[2,4] Ronny P. Bartsch,[2] Jeffrey M. Hausdorff,[5,6] Luís A. Nunes Amaral,[7] Verena Schulte-Frohlinde,[1] H. Eugene Stanley,[1] and Mitsuru Yoneyama[8]

[1]*Department of Physics and Center for Polymer Studies, Boston University, Boston, Massachusetts 02215, USA*

[2]*Harvard Medical School and Division of Sleep Medicine, Brigham and Women's Hospital, Boston, Massachusetts 02115, USA*

[3]*Institute of Solid State Physics, Bulgarian Academy of Sciences, Sofia 1784, Bulgaria*

[4]*Nanjing University of Posts and Telecommunications, Nanjing 210003, China*

[5]*Tel-Aviv Sourasky Medical Center and Tel-Aviv University, Tel-Aviv 69978, Israel*

[6]*Harvard Medical School, Boston, Massachusetts 02115, USA*

[7]*Department of Chemical Engineering, Northwestern University, Evanson, Illinois 60208, USA*

[8]*Mitsubishi Chemical Group, Science and Technology Center Inc., Yokohama 227-8502, Japan*

(Received 5 May 2004; revised manuscript received 3 January 2009; published 21 April 2009)

Many physical and physiological signals exhibit complex scale-invariant features characterized by $1/f$ scaling and long-range power-law correlations, indicating a possibly common control mechanism. Specifically, it has been suggested that dynamical processes, influenced by inputs and feedback on multiple time scales, may be sufficient to give rise to $1/f$ scaling and scale invariance. Two examples of physiologic signals that are the output of hierarchical multiscale physiologic systems under neural control are the human heartbeat and human gait. Here we show that while both cardiac interbeat interval and gait interstride interval time series under healthy conditions have comparable $1/f$ scaling, they still may belong to different complexity classes. Our analysis of the multifractal scaling exponents of the fluctuations in these two signals demonstrates that in contrast to the multifractal behavior found in healthy heartbeat dynamics, gait time series exhibit less complex, close to monofractal behavior. Further, we find strong anticorrelations in the sign and close to random behavior for the magnitude of gait fluctuations at short and intermediate time scales, in contrast to weak anticorrelations in the sign and strong positive correlation for the magnitude of heartbeat interval fluctuations—suggesting that the neural mechanisms of cardiac and gait control exhibit different linear and nonlinear features. These findings are of interest because they underscore the limitations of traditional two-point correlation methods in fully characterizing physiological and physical dynamics. In addition, these results suggest that different mechanisms of control may be responsible for varying levels of complexity observed in physiological systems under neural regulation and in physical systems that possess similar $1/f$ scaling.

DOI: 10.1103/PhysRevE.79.041920 PACS number(s): 87.10.−e, 87.19.Hh, 05.45.Tp, 05.40.−a

I. INTRODUCTION

Many dynamic systems generate outputs with fluctuations characterized by $1/f$-like scaling of the power spectra, $S(f)$, where f is the frequency. These fluctuations are often associated with nonequilibrium dynamic systems possessing multiple degrees of freedom [1,2], rather than being the output of a classic "homeostatic" process [3–5]. It is generally assumed that the presence of many components interacting over a wide range of time or space scales could be the reason for the $1/f$ spectrum in the fluctuations [6,7]. Fluctuations exhibiting $1/f$-like behavior are often termed "complex," since they obey a scaling law indicating a hierarchical fractal organization of their frequency (time scale) components rather than being dominated by a single frequency. $1/f$ behavior is common in a variety of physical, biological, and social systems [7–15]. The ubiquity of the $1/f$ scale-invariant phenomenon has triggered in recent years the development of generic mechanisms describing complex systems, independent of their particular context, in order to understand the "unifying" features of these systems [16–19].

To evaluate whether fluctuations in signals generated by integrated physiological systems exhibit the same level of complexity, we analyze and compare the time series generated by two physiologic control systems under multiple-component integrated neural control—the human gait and the human heartbeat. We chose these two particular examples because human gait and heartbeat control share certain fundamental properties, e.g., both originate in oscillatory centers. In the case of the heart, the pacemaker is located in the sinus node in the right atrium [20]. For gait, pacemakers called central pattern generators are thought to be located in the spinal cord [21].

However, these two systems are distinct suggesting possible dynamical differences in their output. For example, heartbeat fluctuations are primarily controlled by the involuntary (autonomic) nervous system. In contrast, while the spontaneous walking rhythm is an automaticlike process, voluntary inputs play a major role. Further, gait control resides in the basal ganglia and related motor areas of the central nervous system, while the heartbeat is controlled by the sympathetic and parasympathetic branches of the autonomic nervous system [20,22].

Previous studies show comparable two-point linear correlations and $1/f$ power spectra in heart rate [23–27] and human gait [28–31] suggesting that differences in physiologic control may not be manifested in beat-to-beat and interstride interval fluctuations. Recent studies focusing on higher order correlations and nonlinear properties show that the human

*Corresponding author; plamen@buphy.bu.edu

heartbeat exhibits not only $1/f$ fractal but also multifractal properties [32]. Since multifractal signals require many scaling indices to fully characterize their scaling properties, they may be considered to be more complex than those characterized by a single fractal dimension such as classical $1/f$ noise. Although the origins of the multifractal features in heartbeat dynamics are not yet understood, there is evidence that they relate to the complex intrinsic neuroautonomic regulation of the heart [32,33]. Human gait, e.g., free unconstrained walking, is also a physiological process regulated by complex hierarchical feedback mechanisms involving supraspinal inputs [21]. Moreover, recent findings indicate that the scaling properties of gait fluctuations relate to neural centers on the higher supraspinal level rather than to lower motor neurons or environmental inputs [34,35]. Thus, it would be natural to hypothesize that the fluctuations in healthy unconstrained human gait exhibit similar fractal and multifractal features as heartbeat fluctuations, and that human gait dynamics may belong to the same "complexity class" as cardiac dynamics.

We employ two techniques—magnitude and sign decomposition analysis [36,37], and multifractal analysis [38,39]—to probe long-term nonlinear features, and to compare the levels of complexity in heartbeat and interstride interval fluctuations. To this end, we analyze interstride interval time series from ten young healthy men (mean age 22 years) with no history of neuromuscular disorders [40]. Subjects walked continuously for 1 h at a self-selected usual pace on level ground around a flat, obstacle-free, approximately oval, 400 m long path. The interstride interval was measured using a ground reaction force sensor—ultrathin force-sensitive switches were taped inside one shoe and data were recorded on an ambulatory recorder using a previously validated method [41]. We compare the results of our gait analysis with results we have previously obtained [32,36,42,43] from 6-h-long heartbeat interval records from 18 healthy individuals (13 female and 5 male, mean age 34 years) during daily activity (12:00 to 18:00) [40].

As described below, we systematically compare the scaling properties of the fluctuations in human gait with those in the human heartbeat using power spectral analysis, detrended fluctuation analysis (DFA), magnitude, and sign decomposition analysis, and wavelet-based multifractal analysis, and we quantify linear and nonlinear features in the data over a range of time scales.

II. METHODS

A. DFA

The DFA method was developed because conventional fluctuation analyses such as power spectral, R/S and Hurst analysis cannot be reliably used to study nonstationary data [44–48]. One advantage of the DFA method is that it allows the detection of long-range power-law correlations in noisy signals with embedded polynomial trends that can mask the true correlations in the fluctuations of a signal. The DFA method has been successfully applied to a wide range of research fields in physics [49–52], biology [53–56], and physiology [57–60].

The DFA method involves the following steps [44]:

(i) Given the original signal $s(i)$, where $i=1,\ldots,N_{\max}$ and $N_{\max}$ is the length of the signal, we first form the profile function $y(k)\equiv\sum_{i=1}^{k}[s(i)-\langle s\rangle]$, where $\langle s\rangle$ is the mean. One can consider the profile $y(k)$ as the position of a random walk in one dimension after k steps.

(ii) We divide the profile $y(k)$ into nonoverlapping segments of equal length n.

(iii) In each segment of length n, we fit $y(k)$, using a polynomial function of order ℓ which represents the polynomial *trend* in that segment. The y coordinate of the fit line in each segment is denoted by $y_n(k)$. Since we use a polynomial fit of order ℓ, we denote the algorithm as DFA-ℓ.

(iv) The profile function $y(k)$ is detrended by subtracting the local trend $y_n(k)$ in each segment of length n. In DFA-ℓ, trends of order $\ell-1$ in the original signal are eliminated. Thus, comparison of the results for different orders of DFA-ℓ allows us to estimate the type of polynomial trends in the time series $s(i)$.

(v) For a given segment of length n, the root-mean-square (rms) fluctuation for this integrated and detrended signal $s(i)$ is calculated:

$$F(n)\equiv\sqrt{\frac{1}{N_{\max}}\sum_{k=1}^{N_{\max}}[y(k)-y_n(k)]^2}. \tag{1}$$

(vi) Since we are interested in how $F(n)$ depends on the segment length, the above computation is repeated for a broad range of scales n.

A power-law relation between the average root-mean-square fluctuation function $F(n)$ and the segment length n indicates the presence of scaling:

$$F(n)\sim n^{\alpha}. \tag{2}$$

Thus, the DFA method can quantify the temporal organization of the fluctuations in a given signal $s(i)$ by a single scaling exponent α—a self-similarity parameter which represents the long-range power-law correlation properties of the signal. If $\alpha=0.5$, there is no correlation and the signal is uncorrelated (white noise); if $\alpha<0.5$, the signal is anticorrelated; if $\alpha>0.5$, the signal is correlated. The larger the value of α, the stronger the correlations in the signal.

For stationary signals with scale-invariant temporal organization, $F(n)$ is related to the Fourier power spectrum $S(f)$ and to the autocorrelation function $C(n)$. For such signals,

$$S(f)\sim f^{-\beta},\quad \text{where } [\beta=2\alpha-1] \tag{3}$$

and α is the DFA scaling exponent [Eq. (2)] [44]. Thus, signals with $1/f$ scaling in the power spectrum (i.e., $\beta=1$) are characterized by DFA exponent $\alpha=1$. If $0.5<\alpha<1$, the correlation exponent γ describes the decay of the autocorrelation function:

$$C(n)\equiv\langle s(i)s(i+n)\rangle\sim n^{-\gamma},\quad \text{where } [\gamma=2-2\alpha]. \tag{4}$$

B. Magnitude and sign decomposition method

Fluctuations in the dynamical output of physical and physiological systems can be characterized by their magnitude (absolute value) and their direction (sign). These two

quantities reflect the underlying interactions in a given system—the resulting "force" of these interactions at each moment determines the magnitude and the direction of the fluctuations. To assess the information contained in these fluctuations, the magnitude and sign decomposition method was introduced [36,37]. This method involves the following steps:

(i) Given the original signal $s(i)$ we generate the increment series, $\Delta s(i) \equiv s(i+1) - s(i)$.

(ii) We decompose the increment series into a magnitude series $|\Delta s(i)|$ and a sign series $\text{sign}[\Delta s(i)]$.

(iii) To avoid artificial trends we subtract from the magnitude and sign series their average.

(iv) We then integrate both magnitude and sign series, because of limitations in the accuracy of the DFA method for estimating the scaling exponents of anticorrelated signals ($\alpha < 0.5$).

(v) We perform a scaling analysis using second-order detrended fluctuation analysis (DFA-2) on the integrated magnitude and sign series.

(vi) To obtain the scaling exponents for the magnitude and sign series, we measure the slope of $F(n)/n$ on a log-log plot, where $F(n)$ is the root-mean-square fluctuation function obtained using DFA-2 and n is the scale.

Fluctuations following an identical $1/f$ scaling law can exhibit different types of correlations for the magnitude and the sign—e.g., a signal with anticorrelated fluctuations can exhibit positive correlations in the magnitude. Positive correlations in the magnitude series indicate that an increment with large magnitude is more likely to be followed by an increment with large magnitude. Anticorrelations in the sign series indicate that a positive increment in the original signal is more likely to be followed by a negative increment. Further, positive power-law correlations in the magnitude series indicate the presence of long-term *nonlinear* features in the original signal, and relate to the width of the multifractal spectrum [37]. In contrast, the sign series relates to the *linear* properties of the original signal [37]. The magnitude and sign decomposition method is suitable to probe nonlinear properties in short nonstationary signals, such as 1 h interstride interval time series.

C. Wavelet-based multifractal analysis

Previously, analyses of the fractal properties of physiologic fluctuations revealed that the behavior of healthy, free-running physiologic systems may often be characterized as $1/f$-like [19,23–27,29,35,41,61–72]. Monofractal signals (such as classical $1/f$ noise) are homogeneous, i.e., they have the same scaling properties throughout the entire signal [73–75]. Monofractal signals can therefore be indexed by a single exponent: the Hurst exponent H [76].

On the other hand, multifractal signals are nonlinear and inhomogeneous with local properties changing with time. Multifractal signals can be decomposed into many subsets characterized by different *local* Hurst exponents h, which quantify the local singular behavior and relate to the local scaling of the time series. Thus, multifractal signals require many exponents to fully characterize their properties [77]. The multifractal approach, a concept introduced in the context of multiaffine functions [78–81], has the potential to describe a wide class of signals more complex than those characterized by a single fractal dimension.

The singular behavior of a signal $s(t)$ at time t_0 — $|s(t) - P_n(t)| \sim |t - t_0|^{h(t_0)}$ for $t \to t_0$—is characterized by the local Hurst exponent $h(t_0)$ where $n < h(t_0) < n+1$ and $P_n(t)$ is a polynomial fit of order n. To avoid an *ad hoc* choice of the range of time scales over which the local Hurst exponent h is estimated, and to filter out possible polynomial trends in the data which can mask local singularities, we implement a wavelet-based algorithm [39]. Wavelets are designed to probe time series over a broad range of scales and have recently been successfully used in the analysis of physiological signals [82–90]. In particular, recent studies have shown that the wavelet decomposition reveals a robust self-similar hierarchical organization in heartbeat fluctuations, with bifurcations propagating from large to small scales [43,91,92]. To quantify hierarchical cascades in gait dynamics and to avoid inherent numerical instability in the estimate of the local Hurst exponent, we employ a "mean-field" approach—a concept introduced in statistical physics [1]—which allows us to probe the collective behavior of local singularities throughout an entire signal and over a broad range of time scales.

We study the multifractal properties of interstride interval time series by applying the *wavelet transform modulus maxima* (WTMM) method [38,39,93] that has been proposed as a mean-field generalized multifractal formalism for fractal signals. We first obtain the wavelet coefficient at time t_0 from the continuous wavelet transform defined as

$$W_a(t_0) \equiv a^{-1} \sum_{t=1}^{N} s(t) \psi[(t - t_0)/a], \tag{5}$$

where $s(t)$ is the analyzed time series, ψ is the analyzing wavelet function, a is the wavelet scale (i.e., time scale of the analysis), and N is the number of data points in the time series. For ψ we use the third derivative of the Gaussian, thus filtering out up to second-order polynomial trends in the data. We then choose the modulus of the wavelet coefficients at each point t in the time series for a fixed wavelet scale a.

Next, we estimate the partition function

$$Z_q(a) \equiv \sum_i |W_a(t)|^q, \tag{6}$$

where the sum is only over the maxima values of $|W_a(t)|$, and the powers q take on real values. By not summing over the entire set of wavelet transform coefficients along the time series at a given scale a but only over the wavelet transform modulus maxima, we focus on the fractal structure of the temporal organization of the singularities in the signal [93].

We repeat the procedure for different values of the wavelet scale a to estimate the scaling behavior

$$Z_q(a) \sim a^{\tau(q)}. \tag{7}$$

Analogous to what occurs in scale-free physical systems, in which phenomena controlled by the same mechanism over multiple time scales are characterized by scale-independent measures, we assume that the scale-independent measures,

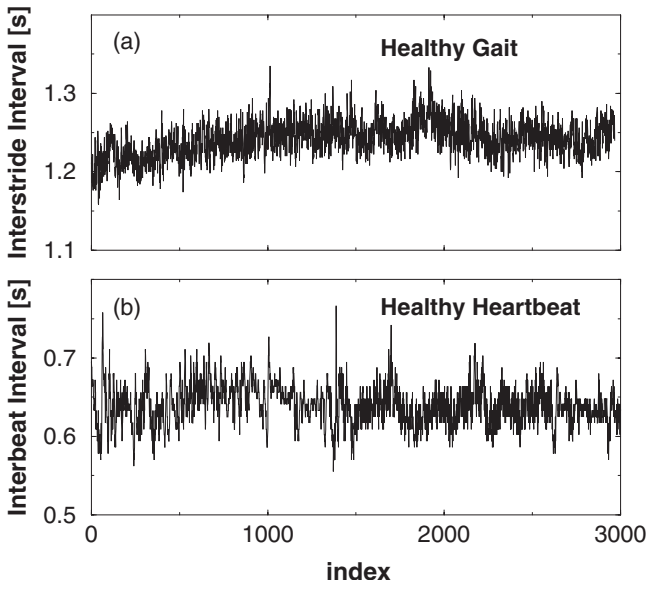

FIG. 1. Representative records of (a) interstride interval (ISI) time series from a healthy subject and (b) consecutive heartbeat (RR) intervals from a healthy subject.

$\tau(q)$, depend only on the underlying mechanism controlling the system. Thus, by studying the scaling behavior of $Z(a,q) \sim a^{\tau(q)}$ we may obtain information about the self-similar (fractal) properties of the mechanism underlying gait control.

For certain values of the powers q, the exponents $\tau(q)$ have familiar meanings. In particular, $\tau(2)$ is related to the scaling exponent of the Fourier power spectra, $S(f) \sim 1/f^{\beta}$, as $\beta = 2 + \tau(2)$ [39]. For positive q, $Z_q(a)$ reflects the scaling of the large fluctuations and strong singularities in the signal, while for negative q, $Z_q(a)$ reflects the scaling of the small fluctuations and weak singularities [74,77,94]. Thus, the scaling exponents $\tau(q)$ can reveal different aspects of the underlying dynamics.

In the framework of this wavelet-based multifractal formalism, $\tau(q)$ is the Legendre transform of the singularity spectrum $D(h)$ defined as the Hausdorff dimension of the set of points t in the signal $s(t)$ where the local Hurst exponent is h. Homogeneous monofractal signals—i.e., signals with a single local Hurst exponent h —are characterized by linear $\tau(q)$ spectrum:

$$\tau(q) = qH - 1, \tag{8}$$

where $H \equiv h = d\tau(q)/dq$ is the global Hurst exponent. On the contrary, a nonlinear $\tau(q)$ curve is the signature of nonhomogeneous signals that display multifractal properties—i.e., $h(t)$ is a varying quantity that depends upon t.

III. RESULTS

In Fig. 1 we show two example time series: (i) an interstride interval time series from a typical healthy subject during ≈ 1 h ($N = 3000$ steps) of unconstrained normal walking on a level, obstacle-free surface [Fig. 1(a)] [40]; (ii) consecutive heartbeat intervals from ≈ 1 h ($N = 3000$ beats) record of a typical healthy subject during daily activity [Fig. 1(b)] [40]. Both time series exhibit irregular fluctuations and nonstationary behavior characterized by different local trends; in fact it is difficult to differentiate between the two time series by visual inspection.

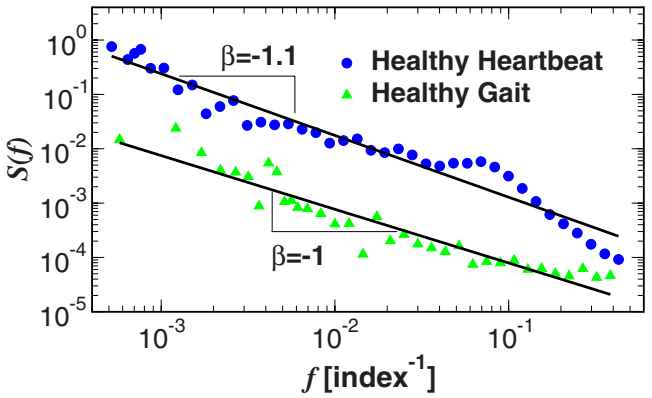

FIG. 2. (Color online) Power spectra of the gait ISI series (▲) and heartbeat RR series (●) displayed in Fig. 1, indicating a similar $1/f$-type behavior.

We first examine the two-point correlations and scale-invariant behavior of the time series shown in Fig. 1. Power spectra $S(f)$ of the gait and heartbeat time series (Fig. 2) indicate that both processes are described by a power-law relation $S(f) \sim 1/f^{\beta}$ over more than 2 decades, with exponent $\beta \approx 1$. This scaling behavior indicates self-similar (fractal) properties of the data over a broad range of time scales, suggestive of an identical level of complexity as quantified by this linear measure. We obtain similar results for the interstride interval time series from all subjects in our gait database: $\beta = 0.9 \pm 0.08$ (group mean $\pm$ std. dev.) in agreement with previous results [35].

A. DFA

Next, to quantify the degree of correlation in the interstride and heartbeat fluctuations we apply the DFA method, which also provides a linear measure: plots of the root-mean-square fluctuation function $F(n)$ vs time scale n (measured in stride or beat number) from a second-order DFA analysis (DFA-2) [44–46] indicate the presence of long-range power-law correlations in both gait and heartbeat fluctuations [Fig. 3(a)]. The scaling exponent $\alpha \approx 0.95$ for the heartbeat signal, shown in Fig. 1(b), is very close to the exponent $\alpha \approx 0.9$ for the interstride interval signal, shown in Fig. 1(a), estimated over the scaling range $6 < n < 600$, where $n_{\max} \approx N/5 = 600$ is the maximal time scale for which the DFA scaling analysis is reliable [45,46]. We obtain similar results for the remaining subjects: $\alpha = 0.87 \pm 0.03$ (group mean $\pm$ std. dev.) for the gait data (in agreement with [35]) and $\alpha = 1.01 \pm 0.06$ for the heartbeat data (in agreement with [42]). The results of both power spectral analysis and the DFA method indicate that gait and heartbeat time series have similar scale-invariant properties suggesting certain parallels in the underlying mechanisms of neural regulation.

B. Magnitude and sign decomposition method

To probe for long-term nonlinear features in the dynamics of interstride intervals we employ the magnitude and sign

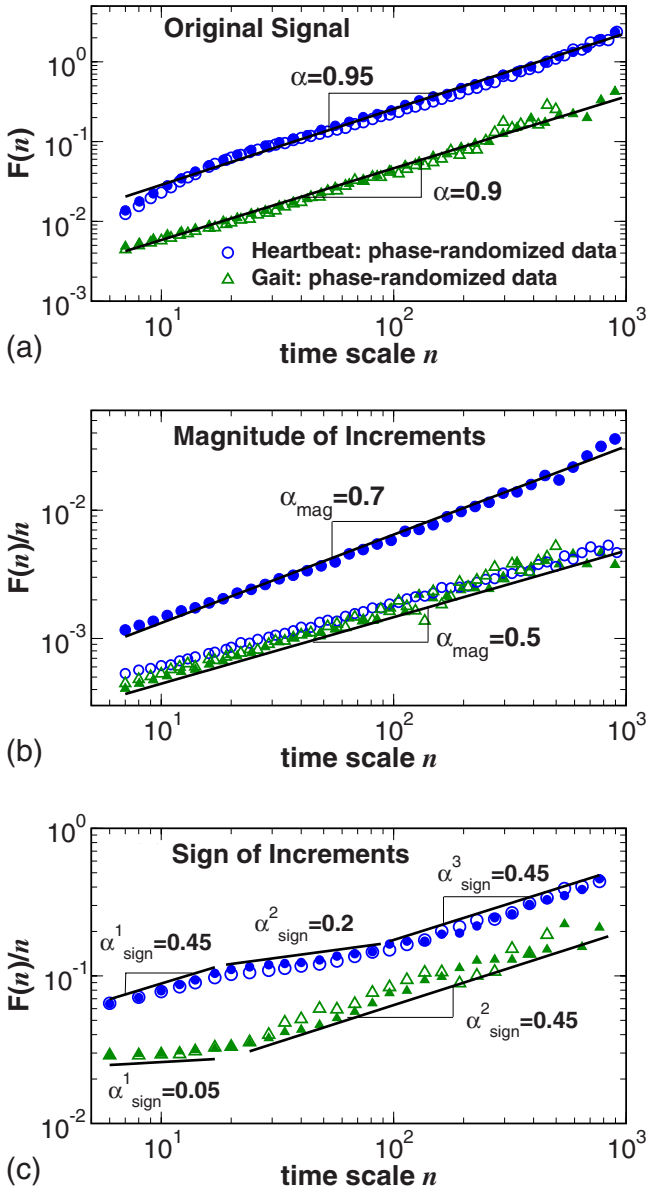

FIG. 3. (Color online) Plots of the root-mean-square fluctuation function $F(n)$ vs time scale n (measured in interstride or heartbeat number) from second-order DFA-2 analysis for (a) the gait ISI (▲) and heartbeat RR (●) time series, (b) the magnitude series, and (c) sign series of the interstride and heartbeat increments ΔISI and ΔRR. The results shown in (a), (b), and (c) are obtained for the gait and heartbeat signals displayed in Figs. 1(a) and 1(b). While both gait and cardiac dynamics exhibit similar power-law and correlations, the magnitude and sign series of interstride and heartbeat increments in (b) and (c) follow significantly different scaling relations. Open symbols (△, ○) represent the results of a Fourier phase-randomization test indicating high degree of nonlinearity ($\alpha_{\text{mag}} \approx 0.7 > 0.5$) in cardiac dynamics, in contrast to a linear behavior ($\alpha_{\text{mag}} \approx 0.5$) for gait dynamics.

decomposition analysis [36,37]. Previous studies have demonstrated that information about the nonlinear properties of heartbeat dynamics can be quantified by long-range power-law correlations in the magnitude of the increments in heartbeat intervals [36]. Further, *positive* correlations in the magnitude are associated with *nonlinear* features in the underlying dynamics. In contrast, *linear* signals are characterized by an absence of correlations (*random* behavior) in the magnitude series. To quantify the correlations in the magnitude of the interstride increments we apply the DFA-2 method to the gait data displayed in Fig. 1(a). Our results show that the magnitude series of the interstride increments exhibits close to random behavior with correlation exponent $\alpha_{\text{mag}} \approx 0.5$ [denoted by (▲) in Fig. 3(b)] suggesting linear properties of the underlying dynamics. In contrast, for the heartbeat data displayed in Fig. 1(b), we find that the magnitude series of the interbeat interval fluctuations exhibits strong positive correlations over more than two decades characterized by exponent $\alpha_{\text{mag}} \approx 0.7$ [denoted by (●) in Fig. 3(b)] suggesting nonlinear features in cardiac control. Thus, the striking difference in the magnitude correlations of gait and heartbeat dynamics (both of which are under multilevel neural control) raises the possibility that these two physiologic processes belong to different classes of complexity whereby the neural regulation of the heartbeat is inherently more nonlinear, over a range of time scales, than the neural mechanism of gait control. Our observation of a low degree of nonlinearity in the gait time series is supported by the remaining subjects in the group: over time scales $6 < n < 600$, we obtain exponent $\alpha_{\text{mag}} = 0.51 \pm 0.03$ (group mean ± std. dev.) for the gait time series, which is significantly lower than the corresponding exponent $\alpha_{\text{mag}} = 0.71 \pm 0.09$ obtained for the heartbeat data ($p = 2.7 \times 10^{-7}$, by the Student's t test). We note however, in the short-range region for time scales $6 < n < 16$ we obtain a group average exponent $\alpha_{\text{mag}} = 0.62 \pm 0.05$ for the gait data, and $\alpha_{\text{mag}} = 0.57 \pm 0.12$ for the heartbeat data (Table I), indicating a very similar (and relatively low) degree of nonlinearity in both gait and cardiac dynamics at short time scales of up to ≈15 s (with p −value=0.16 by the Student's t test). This nonlinear behavior changes significantly at intermediate and large time scales, where cardiac dynamics is characterized by a high degree of nonlinearity ($\alpha_{\text{mag}} \approx 0.8$), in contrast to gait dynamics which exhibits practically linear behavior ($\alpha_{\text{mag}} \approx 0.5$) (see Table I).

To further test for nonlinear features in the mechanisms of neural control generating heartbeat and gait dynamics we perform a Fourier phase-randomization surrogate test [95,96]. We first perform a Fourier transform of the original data. Next we eliminate the nonlinearity in the data by randomizing the Fourier phases while preserving the Fourier coefficients, and thus keeping the linear properties (power spectrum and correlation) of the original signal unchanged. An inverse Fourier transform leads to a linearized surrogate signal with identical correlations as in the original data.

The results of Fourier phase-randomization test for gait and heartbeat data are shown in Fig. 3. While the DFA scaling curves remain as expected, unchanged after the test for both gait and heartbeat signals [Fig. 3(a), open symbols], the scaling curve for the magnitude of heartbeat fluctuations changes dramatically to $\alpha \approx 0.5$, in contrast to the gait data, where the magnitude scaling curve remains practically unchanged [Fig. 3(b), open symbols]. These findings confirm our results from the magnitude analysis indicating that the multilevel neural control mechanism of gait surprisingly generates close to linear dynamics.

TABLE I. Results of the DFA analysis of the original gait ISI and heartbeat RR interval signals, and the magnitude and sign of interstride and heartbeat interval increments, ΔISI and ΔRR for 1 h gait recordings from ten healthy subjects and 6 h ECG recordings from 18 healthy subjects. We calculate the scaling exponents α over a broad range of time scales $6<n\leq 600$, as well as in three different regions: (i) the short-range regime for time scales $6<n<16$ with scaling exponent α_1, (ii) the intermediate regime for time scales $16\leq n\leq 64$ with scaling exponent α_2, (iii) and the long-range regime for time scales $64<n\leq 600$ with scaling exponent α_3. For each measure, the group average ± 1 standard deviation is presented.

Measure	Original	Magnitude	Sign
	Gait		
α	0.87 ± 0.03	0.51 ± 0.03	0.41 ± 0.05
α_1	0.71 ± 0.08	0.62 ± 0.05	0.05 ± 0.03
α_2	0.84 ± 0.06	0.53 ± 0.07	0.40 ± 0.03
α_3	0.89 ± 0.06	0.50 ± 0.08	0.48 ± 0.12
	Heartbeat		
α	1.01 ± 0.06	0.71 ± 0.09	0.35 ± 0.03
α_1	1.34 ± 0.22	0.57 ± 0.12	0.45 ± 0.13
α_2	0.97 ± 0.12	0.67 ± 0.09	0.23 ± 0.08
α_3	1.02 ± 0.10	0.80 ± 0.12	0.45 ± 0.05

Previous studies have shown that the time series composed of the sign of the consecutive increments in the original signal contain information about the underlying dynamics which is complementary and independent from the original and the magnitude series [36,37,97,98]. Our DFA scaling analysis of the sign series shows a complex and significantly different behavior for heartbeat and gait dynamics. A very strong anticorrelated behavior at small time scales with $\alpha_{\text{sign}}\approx 0.05$ is followed by a crossover to much weaker anticorrelations with $\alpha_{\text{sign}}\approx 0.45$ as shown in Fig. 3(c) for the gait data displayed in Fig. 1(a). This is in contrast to the scaling behavior of the heartbeat sign series, which exhibits weak anticorrelations ($\alpha_{\text{sign}}\approx 0.45$) at both short and long time scales with a crossover region at intermediate scales [Fig. 3(c)]. These observations are supported by the remaining subjects in the group: over time scales $6<n<16$, we obtain exponent $\alpha_{\text{sign}}=0.05\pm0.03$ (group mean $\pm$ std. dev.) for gait, which is significantly different from the corresponding exponent $\alpha_{\text{sign}}=0.45\pm0.13$ for heartbeat data ($p-$value $=10^{-9}$ by the Student's t test). At long time scales of $n>100$ both interstride and heartbeat intervals are characterized by a group average exponent $\alpha_{\text{sign}}=0.45$ with a $p-$value$=0.46$ by the Student's t test (see Table I).

Further, our analysis of the sign series from surrogate data obtained after Fourier phase randomization of the original gait and heartbeat signals indicates no change in the scaling behavior [Fig. 3(c), open symbols], suggesting that, in contrast to the magnitude series, correlations in the sign series reflect linear properties in the original data.

Our DFA, and magnitude and sign decomposition analyses show a consistent scaling behavior of gait dynamics for all 10 subjects in our database. All individual scaling curves

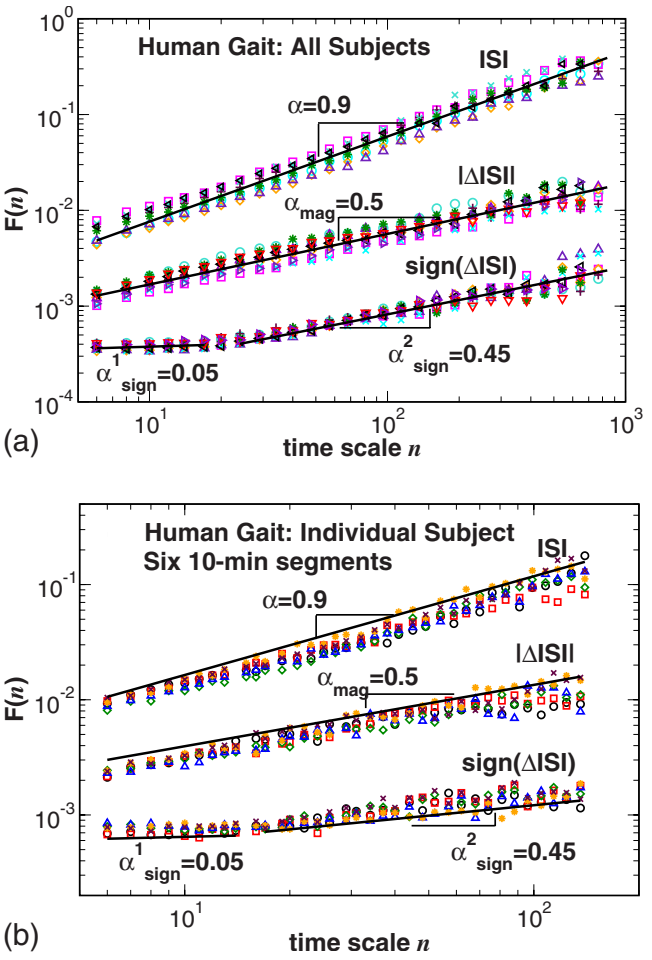

FIG. 4. (Color online) DFA-2 analysis of the gait interstride intervals (ISI) series, the magnitude series $|\Delta\text{ISI}|$ and the sign series sign(ΔISI) for (a) all ten subjects in our database and (b) six 10 min segments of a 1 h recording from one individual subject. A consistent scaling behavior is observed for all subjects as well as for different segments from individual recordings despite certain differences in the average and standard deviation of ISI among subjects and across segments.

for the interstride interval signals, magnitude and sign series practically collapse onto a single curve [Fig. 4(a)]. To further test the validity of our results for gait dynamics, and that they indeed represent the internal mechanics of gait control, and are not an artifact of external/random factors of the environment, we have segmented each 1 h gait recording into 10 min segments, and have separately analyzed each segment. While the average gait rate and standard deviation change for different segments with some subjects reporting a certain degree of fatigue or tiredness near the end of the recording, our results demonstrate a remarkable stability of the scaling results with no statistically significant change in the exponent α, α_{mag}, and α_{sign} for different segments [Fig. 4(b)].

C. Wavelet-based multifractal analysis

To further test the long-term nonlinear features in gait dynamics we study the multifractal properties of interstride

time series. We apply the WTMM method [39,93]—a "mean-field" type approach to quantify the fractal organization of singularities in the signal. We characterize the multifractal properties of a signal over a broad range of time scales by the multifractal spectrum $\tau(q)$. Gait and heartbeat time series contain densely packed, nonisolated singularities which unavoidably affect each other in the time-frequency decomposition. Therefore, rather than evaluating the distribution of the inherently unstable local singularity exponents [14,43]), we estimate the scaling of an appropriately chosen global measure: the q moments of the probability distribution of the maxima of the wavelet transform $Z_q(a)$ (using the third derivative of the Gaussian function as the analyzing wavelet).

We first examine the time series shown in Fig. 1. For the gait time series, we obtain a $\tau(q)$ spectrum which is practically a linear function of the moment q suggesting that the gait dynamics exhibit *monofractal* properties [Figs. 5(a) and 5(c)]. This is in contrast with the nonlinear $\tau(q)$ spectrum for the heartbeat signal [Figs. 5(b) and 5(c)] which is indicative of nonlinear multifractal behavior [38,39]. Further, when analyzing the remaining interstride interval recordings, we find close to linear $\tau(q)$ spectra for all subjects in the gait group [Fig. 6(a)]. Calculating the group averaged $\tau(q)$ spectra we find clear differences: multifractal behavior for the heartbeat dynamics and practically monofractal behavior for the gait dynamics [Fig. 6(b)]. Specifically, we find significant differences between the gait and heartbeat $\tau(q)$ spectra for negative values of the moment q; for positive values of q, the scaling exponents $\tau(q)$ take on similar values. This is in agreement with the similarity in power spectral and DFA scaling exponents for gait and heartbeat data, which correspond to $\tau(q=2)$ (Fig. 3). However, the heartbeat $\tau(q)$ spectrum is visibly more curved for all moments q compared with the gait $\tau(q)$ spectrum which may be approximately fit by a straight line, indicative of a low degree of nonlinearity in the interstride time series. Thus, our results show consistent differences between the nonlinear and multifractal properties of gait and heartbeat time series.

Previous studies have shown that reducing the level of physical activity under a constant routine protocol does not change the multifractal features of heartbeat dynamics, while blocking the sympathetic or parasympathetic tone of the neuroautonomic regulation of the heart dramatically changes the multifractal spectrum, thus suggesting that the observed features in cardiac dynamics arise from the intrinsic mechanisms of control [33]. Similarly, by eliminating polynomial trends in the interstride interval time series corresponding to changes in the gait pace using DFA and wavelet analyses, we find scaling features which remain invariant among individuals. Therefore, since different individuals experience different extrinsic factors, the observed lower degree of nonlinearity (as measured by the magnitude scaling exponent) and the close-to-monofractal behavior (characterized by practically linear $\tau(q)$ spectrum) appear to be a result of the intrinsic mechanisms of gait regulation. These observations suggest that while both gait and heartbeat dynamics arise from layers of neural control with multiple component interactions, and exhibit temporal organization over multiple time scales, they nonetheless belong to different complexity classes. While

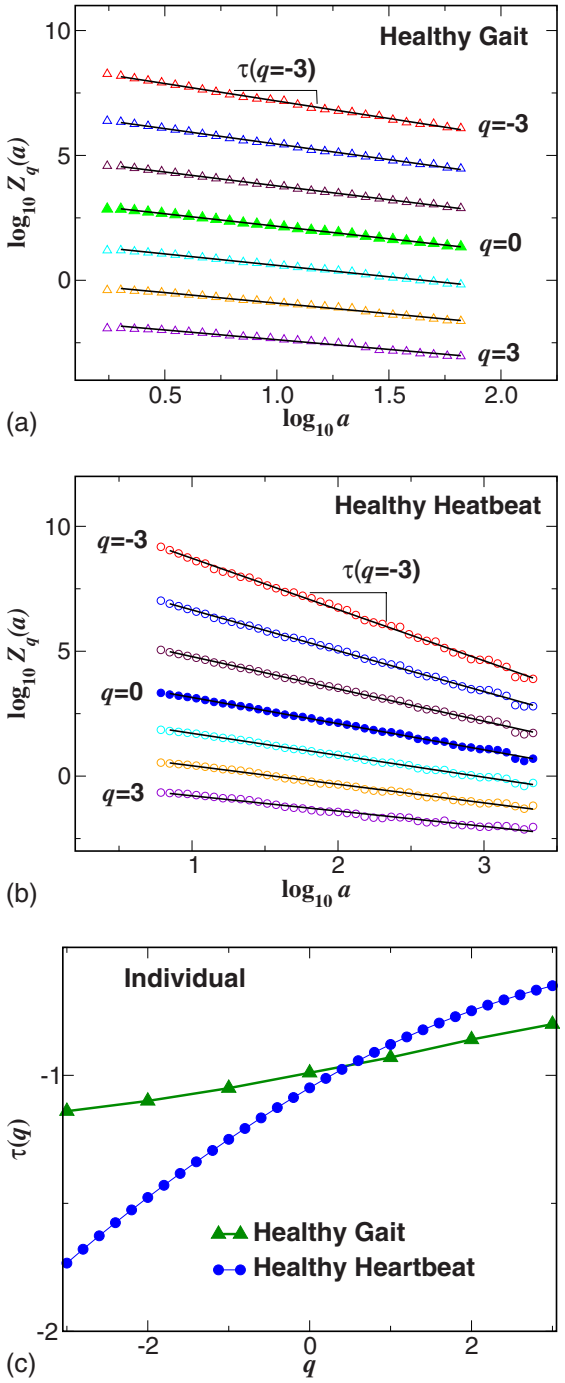

FIG. 5. (Color online) Multifractal analysis: Scaling of the partition function $Z_q(a)$ of the wavelet-transform modulus maxima obtained using the third derivative of the Gaussian as a wavelet function for (a) an individual ISI gait recording, and (b) an individual RR heartbeat recording. (c) Multifractal spectrum $\tau(q)$ for the individual records shown in (a) and (b), where τ is a scaling index associated with different moments q [Eq. (7)]. A monofractal signal corresponds to a straight line for $\tau(q)$, while for multifractal signals $\tau(q)$ is a nonlinear function of q. Thus, our results indicate multifractal/nonlinear behavior in heartbeat dynamics in contrast to monofractal/linear behavior in gait. Note that the values of $\tau(q=2)$ for both gait and heartbeat time series are very close, in agreement with our findings based on DFA-2 correlation analysis [Fig. 3(a)].

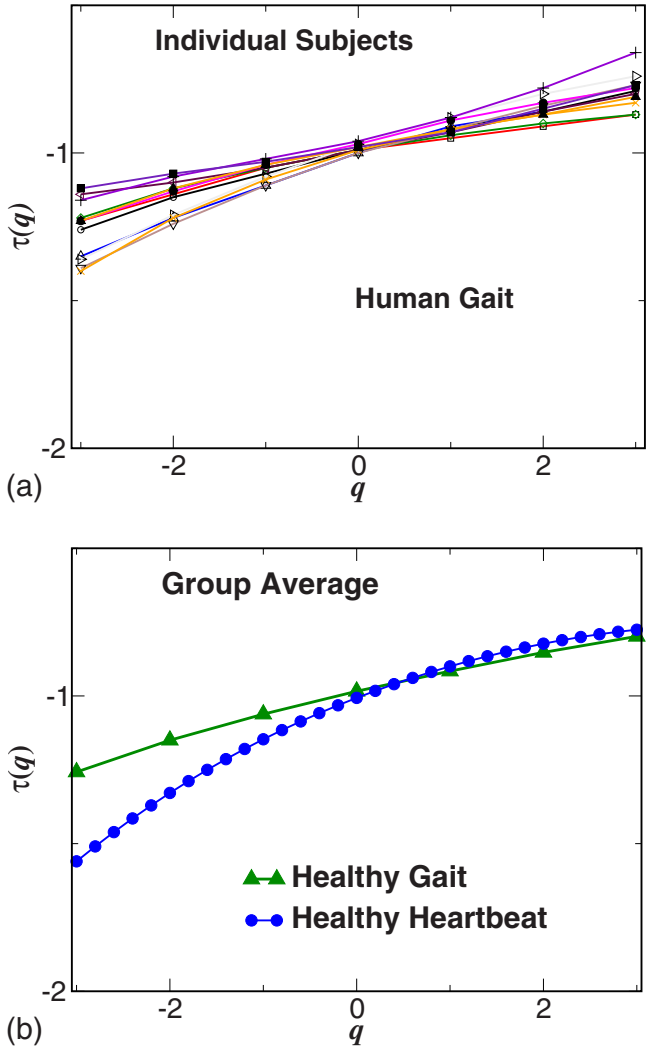

FIG. 6. (Color online) Multifractal analysis: (a) Multifractral spectra $\tau(q)$ for all ten subjects in our gait database [40] exhibit close to linear dependence on the moment q, suggesting monofractal behavior, in contrast to the nonlinear $\tau(q)$ spectra reported for heartbeat recordings [99]. (b) Group average multifractal spectra $\tau(q)$ for the gait and heartbeat subjects in our database [40]. The results show a consistent monofractal (almost linear) behavior for the gait time series, in contrast with the multifractal behavior of the heartbeat data.

both gait and heartbeat dynamics may be a result of competing inputs interacting through multiple feedback loops, differences in the nature of these interactions may be imprinted in their nonlinear and multifractal features: namely, our findings suggest that while these interactions in heartbeat dynamics are of a nonlinear character and are represented by Fourier phase correlations encoded in the magnitude scaling and the multifractal spectrum, feedback mechanisms of gait dynamics lead to decreased interactions among the Fourier phases.

D. Further validation of gait results

These findings are supported by our analysis of a second group of gait subjects. We analyze interstride intervals from an additional group of seven young healthy subjects (six male, one female, mean age 28 years) recorded using a portable accelerometer [100]. Subjects walked continuously for ≈ 1 h at a self-selected pace on an unconstrained outdoor walking track in a park environment allowing for slight changes in elevation and obstacles related to pedestrian traffic. The stride interval time series in this case were obtained from peak-to-peak intervals in the accelerometer signal output in the direction of the subjects' vertical axis. The accelerometer device we used ($9 \times 6 \times 2$ cm, weight 140 g) was developed by Sharp Co. The device, attached to subjects' back, measures the vertical and anteroposterier acceleration profile during walking. The output signals are digitized at a sampling frequency of 10^3 Hz, and are stored on a memory card. When the subjects' heel strikes the ground, a clear peak in the acceleration along the vertical axis is recorded. The positions of these peaks in time are also verified independently through matching steepest points in the anteroposterier acceleration signal output. Our analysis indicates a compatibility of the ground reaction force sensor, used for the gait recordings of the first group [40,41], with the accelerometer device used for the second group [100], as well as a strong correlation between the outputs of the two devices.

We find that for the second gait group the two-point correlation exponent $\alpha = 0.90 \pm 0.1$ (group mean $\pm$ std. dev.), as measured by the DFA-2 method in the range of time scales $6 < n < 600$ is similar to the group average exponent of the first gait group ($\alpha = 0.87 \pm 0.03$) and also to the heartbeat data ($\alpha = 1.01 \pm 0.08$). In contrast, we find again a significantly lower degree of nonlinearity, as measured by the group average magnitude exponent $\alpha_{\mathrm{mag}} = 0.57 \pm 0.04$ in the range of time scales $6 < n < 600$ and by the $\tau(q)$ spectrum, compared with heartbeat dynamics $\alpha_{\mathrm{mag}} = 0.71 \pm 0.06$ ($p = 1.3 \times 10^{-3}$, by the Student's t test). On the other hand, the group averaged value of $\alpha_{\mathrm{mag}} = 0.57 \pm 0.04$ for the second gait group is slightly higher compared to $\alpha_{\mathrm{mag}} = 0.51 \pm 0.03$ for the first gait group, and this is associated with slightly stronger curvature in the $\tau(q)$ spectrum for the second gait group. This may be attributed to the fact that the second group walked in a natural park environment where obstacles, changes in elevation and pedestrian traffic may possibly require the activation of higher neural centers of gait control.

To test to what extent our results depend on the order of polynomial detrending used in the DFA method, we have repeated our analyses using different orders DFA: DFA-1 which removes constant trends in the analyzed signal, DFA-2 which removes both constant and linear trends, and DFA-3 removing constant, linear and quadratic trends. While there is a measurable difference in the results for the scaling exponent α obtained from DFA-1 compared to DFA-2 ($\approx 3\%$ difference, with higher values for α from DFA-1), we find practically identical results for the exponent α obtained from DFA-2 and DFA-3 ($\approx 1\%$ difference in α), suggesting that removing polynomial trends of second and higher order in the recordings does not lead to significantly different scaling results (see Fig. 7). The same is also valid when wavelets with higher than third-order derivatives of the Gaussian are used for the multifractal analysis in Sec. III C.

The present results are related to a physiologically-based model of gait control where specific interactions between

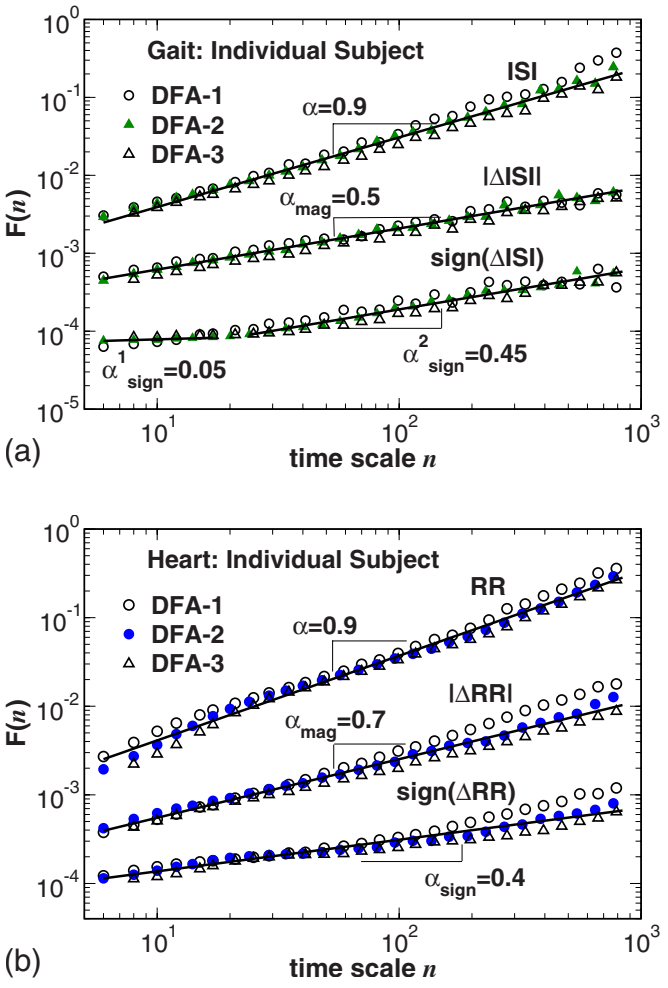

FIG. 7. (Color online) Results of DFA-l analysis with different order $l=1,2,3$ of polynomial detrending for (a) gait and (b) heartbeat data. Note that DFA-l removes trends of order up to $(l-1)$ in the time series. Considering the group average $\langle \Delta\alpha \rangle_i$ of the differences $\Delta\alpha^i_{1,2} \equiv \alpha^i(\text{DFA}-1) - \alpha^i(\text{DFA}-2)$, where i indicates different subjects, we obtain the following: for the original interstride signal $\langle \Delta\alpha_{1,2} \rangle_i = 0.03 \pm 0.03$ and $\langle \Delta\alpha_{2,3} \rangle_i = 0.007 \pm 0.009$, indicating that the results obtained from DFA-2 and DFA-3 are *not* significantly different. Thus, using higher order of polynomial detrending does not change the scaling result, i.e., compared to constant and linear trends, quadratic trends do not contribute significantly to the nonstationarity of gait. These observations remain valid also for the magnitude and sign scaling analysis as shown in (a) and (b).

neural centers are considered [12,13]. In this model a lower degree of nonlinearity (and close-to-linear monofractal $\tau(q)$ spectrum) reflects increased connectivity between neural centers, typically associated with maturation of gait dynamics in adults. The present results are also consistent with studies that used a different approach to quantify the dynamics of gait, based on estimates of the local Hurst exponents, and reported only weak multifractality in gait dynamics [14,15].

IV. SUMMARY

In summary, we find that while the fluctuations in the output of both gait and heartbeat processes are characterized by similar two-point correlation properties and $1/f$-like power spectra, they belong to different classes of complexity—human gait fluctuations exhibit practically linear $\tau(q)$ spectrum and close to monofractal properties characterized by a single scaling exponent, while heartbeat fluctuations exhibit nonlinear multifractal properties, which in physical systems have been connected with turbulence and related multiscale phenomena [32,38,43,80,81,101]. Our analyses indicate that while two systems—cardiac and locomotion, both under integrated neural control and with multicomponent feedback interactions over a range of time scales—can be characterized by long-range power-law correlations of $1/f$-type, other linear and nonlinear scaling features of their dynamics can be markedly different. This study demonstrates that different combinations of scaling behavior for the magnitude and sign of the fluctuations can lead to similar scaling behavior over a broad range of time scales in the correlations of the fluctuations in the output of these systems. Specifically, we find strong anticorrelations in the sign and close to random behavior for the magnitude of gait fluctuations at short and intermediate time scales, in contrast to weak anticorrelations in the sign and strong positive correlation for the magnitude of heartbeat interval fluctuations—suggesting that, despite certain similarities, these physiologic systems belong to different subclasses of complexity.

We note that, our observations of higher than 0.5 values for the gait magnitude exponent $\alpha_{\text{mag}} \approx 0.6$ at short time scales of up to 15 s (Table I) are in agreement with earlier reports of slightly nonlinear/multifractal behavior in gait dynamics based on estimates of the local Hölder exponents [14]. This slightly multifractal behavior at short time scales—which may result from (i) the inherent instability of nonisolated local singularities in gait fluctuations as quantified by the local Hölder exponents or (ii) may be intrinsically related to local nonlinear Fourier-phase correlations in gait dynamics—appears to be lost at time scales above 15 s, where the global scaling exponent $\alpha_{\text{mag}} \approx 0.5$ (Table I), and the multifractal spectrum $\tau(q)$ appears linear for different moments q (Fig. 5). Our observation of a transition in gait dynamics from slightly nonlinear (at short time scales) to linear/monofractal behavior (at long time scales) relates to earlier empirical and modeling studies reporting (i) a decrease in long-term gait nonlinearity, as measured by α_{mag}, with maturation from childhood to adulthood, and (ii) that this decrease in nonlinearity/multifractality with age may be related to increased connectivity (i.e., ability to operate over a broader range of frequency/time scales) among the central pattern generators responsible for gait control at different frequency modes [13].

We further note that different mechanisms may be involved in various aspects of locomotor control. For example, in contrast to gait dynamics where we observe $\alpha_{\text{mag}} \approx 0.5$ indicating linear behavior, our prior studies of forearm motion [102,103] show $\alpha_{\text{mag}} \approx 0.8$, indicating high degree of nonlinearity in wrist activity dynamics, although both gait and wrist dynamics are characterized by identical long-range power-law correlations with an exponent $\alpha \approx 0.9$ [12,13,102,103]. Thus, comparing the "mosaic" of scaling, nonlinear, and multifractal measures of gait interstride inter-

vals with similar measures of other physiologic systems is necessary for better understanding the dynamics of these systems and for further developing more adequate models of integrated neural control [104–106].

The findings reported here are of interest because they underscore the limitations of traditional two-point correlation methods in characterizing physiological and physical time series. In addition, these results suggest that feedback on multiple time scales is not sufficient to explain different types of $1/f$ scaling and scale invariance, and highlight the need for the development of new models [107–110] that could account for the scale-invariant outputs of different types of feedback systems.

ACKNOWLEDGMENTS

This work was supported by grants from Mitsubishi Chemical Co., Yokahama, Japan, NIH/National Center for Research Resources (Grants No. P41 RR13622 and AG14100) and NIH (Grant No. HL071972). We thank Yosef Ashkenazy and Ainslie Yuen for helpful discussions.

[1] H. E. Stanley, *Introduction to Phase Transitions and Critical Phenomena* (Oxford University Press, New York, 1971).
[2] P. Bak and M. Creutz, *Fractals in Science*, edited by A. Bunde and S. Havlin (Springer-Verlag, Berlin, 1994).
[3] C. Bernard, *Leçons sur les Phénoménes de la Vie Communs aux Animaux et aux Végétaus* (Baillière, Paris, 1878), Vols. 1 and 2.
[4] B. van der Pol and J. van der Mark, Philos. Mag. **6**, 763 (1928).
[5] W. B. Cannon, Physiol. Rev. **9**, 399 (1929).
[6] J. B. Johnson, Phys. Rev. **26**, 71 (1925).
[7] P. Dutta and P. M. Horn, Rev. Mod. Phys. **53**, 497 (1981).
[8] *Ninth International Symposium on Noise in Physical Systems*, edited by C. M. Van Vliet (World Scientific, Singapore, 1987).
[9] M. B. Weissman, Rev. Mod. Phys. **60**, 537 (1988).
[10] T. Musha and H. Higuchi, Jpn. J. Appl. Phys. **15**, 1271 (1976).
[11] Y. Liu, P. Gopikrishnan, P. Cizeau, M. Meyer, C.-K. Peng, and H. E. Stanley, Phys. Rev. E **60**, 1390 (1999).
[12] J. M. Hausdorff, Y. Ashkenazy, C.-K. Peng, P. Ch. Ivanov, H. E. Stanley, and A. L. Goldberger, Physica A **302**, 138 (2001).
[13] Y. Ashkenazy, J. M. Hausdorff, P. Ch. Ivanov, and H. E. Stanley, Physica A **316**, 662 (2002).
[14] N. Scafetta, L. Griffin, and B. J. West, Physica A **328**, 561 (2003).
[15] B. J. West and N. Scafetta, Phys. Rev. E **67**, 051917 (2003).
[16] M. F. Shlesinger, Ann. N. Y. Acad. Sci. **504**, 214 (1987).
[17] M. F. Shlesinger and B. J. West, *Random Fluctuations and Pattern Growth: Experiments and Models*, edited by H. E. Stanley and N. Ostrowsky (Kluwer Academic, Boston, 1988).
[18] B. J. West and M. F. Shlesinger, Int. J. Mod. Phys. B **3**, 795b (1989).
[19] J. B. Bassingthwaighte, L. S. Liebovitch, and B. J. West, *Fractal Physiology* (Oxford University Press, New York, 1994); L. S. Liebovitch and T. I. Toth, Ann. N.Y. Acad. Sci. **591**, 375 (1990).
[20] R. M. Berne and M. N. Levy, *Cardiovascular Physiology*, 6th ed. (C.V. Mosby, St. Louis, 1996).
[21] V. T. Inman, H. J. Ralston, and F. Todd, *Human Walking* (Williams and Wilkins, Baltimore, 1981).
[22] M. N. Levy, Circ. Res. **29**, 437 (1971).
[23] M. Kobayashi and T. Musha, IEEE Trans. Biomed. Eng. **BME-29**, 456 (1982).
[24] Y. Yamamoto and R. L. Hughson, J. Appl. Physiol. **71**, 1143 (1991).
[25] Y. Yamamoto and R. L. Hughson, Physica D **68**, 250 (1993).
[26] C.-K. Peng, J. Mietus, J. M. Hausdorff, S. Havlin, H. E. Stanley, and A. L. Goldberger, Phys. Rev. Lett. **70**, 1343 (1993).
[27] *Heart Rate Variability*, edited by M. Malik and A. J. Camm (Futura, Armonk, NY, 1995).
[28] M. P. Kadaba, H. K. Ramakrishnan, M. E. Wootten, J. Gainey, G. Gorton, and G. V. B. Cochran, J. Orthop. Res. **7**, 849 (1989).
[29] J. M. Hausdorff, C.-K. Peng, Z. Ladin, J. Y. Wei, and A. L. Goldberger, J. Appl. Physiol. **78**, 349 (1995).
[30] H. Yang, F. Zhao, Y. Zhuo, X. Wu, and Z. Li, Physica A **312**, 23 (2002).
[31] J. M. Hausdorff, Hum. Mov. Sci. **26**, 555 (2007).
[32] P. Ch. Ivanov, L. A. N. Amaral, A. L. Goldberger, S. Havlin, M. G. Rosenblum, Z. Struzik, and H. E. Stanley, Nature (London) **399**, 461 (1999).
[33] L. A. N. Amaral, P. Ch. Ivanov, N. Aoyagi, I. Hidaka, S. Tomono, A. L. Goldberger, H. E. Stanley, and Y. Yamamoto, Phys. Rev. Lett. **86**, 6026 (2001).
[34] J. J. Collins and I. Stewart, Biol. Cybern. **68**, 287 (1993).
[35] J. M. Hausdorff, P. L. Purdon, C.-K. Peng, Z. Ladin, J. Y. Wei, and A. L. Goldberger, J. Appl. Physiol. **80**, 1448 (1996).
[36] Y. Ashkenazy, P. Ch. Ivanov, S. Havlin, C.-K. Peng, A. L. Goldberger, and H. E. Stanley, Phys. Rev. Lett. **86**, 1900 (2001).
[37] Y. Ashkenazy, S. Havlin, P. Ch. Ivanov, C.-K. Peng, V. Schulte-Frohlinde, and H. E. Stanley, Physica A **323**, 19 (2003).
[38] J. F. Muzy, E. Bacry, and A. Arneodo, Phys. Rev. Lett. **67**, 3515 (1991).
[39] J. F. Muzy, E. Bacry, and A. Arneodo, Int. J. Bifurcat. Chaos **4**, 245 (1994).
[40] Gait Database available at http://www.physionet.org/; MIT-BIH Normal Sinus Rhythm Database available at http://www.physionet.org/physiobank/database/ecg
[41] J. M. Hausdorff, Z. Ladin, and J. Y. Wei, J. Biomech. **28**, 347 (1995).
[42] P. Ch. Ivanov, A. Bunde, L. A. N. Amaral, S. Havlin, J. Fritsch-Yelle, R. M. Baevsky, H. E. Stanley, and A. L. Goldberger, Europhys. Lett. **48**, 594 (1999).
[43] P. Ch. Ivanov, L. A. N. Amaral, A. L. Goldberger, S. Havlin, M. G. Rosenblum, H. E. Stanley, and Z. Struzik, Chaos **11**, 641 (2001).
[44] C.-K. Peng, S. V. Buldyrev, S. Havlin, M. Simons, H. E. Stan-

ley, and A. L. Goldberger, Phys. Rev. E **49**, 1685 (1994).
[45] K. Hu, P. Ch. Ivanov, Z. Chen, P. Carpena, and H. E. Stanley, Phys. Rev. E **64**, 011114 (2001).
[46] Z. Chen, P. Ch. Ivanov, K. Hu, and H. E. Stanley, Phys. Rev. E **65**, 041107 (2002).
[47] L. Xu, P. Ch. Ivanov, K. Hu, Z. Chen, A. Carbone, and H. E. Stanley, Phys. Rev. E **71**, 051101 (2005).
[48] Z. Chen, K. Hu, P. Carpena, P. Bernaola-Galvan, H. E. Stanley, and P. Ch. Ivanov, Phys. Rev. E **71**, 011104 (2005).
[49] N. Vandewalle, M. Ausloos, M. Houssa, P. W. Mertens, and M. M. Heyns, Appl. Phys. Lett. **74**, 1579 (1999).
[50] K. Ivanova and M. Ausloos, Physica A **274**, 349 (1999).
[51] A. Montanari, R. Rosso, and M. S. Taqqu, Water Resour. Res. **36**, 1249 (2000).
[52] B. D. Malamud and D. L. Turcotte, J. Stat. Plan. Infer. **80**, 173 (1999).
[53] S. V. Buldyrev, A. L. Goldberger, S. Havlin, C.-K. Peng, H. E. Stanley, and M. Simons, Biophys. J. **65**, 2673 (1993).
[54] S. M. Ossadnik, S. B. Buldyrev, A. L. Goldberger, S. Havlin, R. N. Mantegna, C.-K. Peng, M. Simons, and H. E. Stanley, Biophys. J. **67**, 64 (1994).
[55] M. S. Taqqu, V. Teverovsky, and W. Willinger, Fractals **3**, 785 (1995).
[56] S. Havlin, S. V. Buldyrev, A. L. Goldberger, R. N. Mantegna, C.-K. Peng, M. Simons, and H. E. Stanley, Fractals **3**, 269 (1995).
[57] D. T. Schmitt and P. Ch. Ivanov, Am. J. Physiol. **293**, R1923 (2007).
[58] T. H. Makikallio, J. Koistinen, L. Jordaens, M. P. Tulppo, N. Wood, B. Golosarsky, C.-K. Peng, A. L. Goldberger, and H. V. Huikuri, Am. J. Cardiol. **83**, 880 (1999).
[59] A. Bunde, S. Havlin, J. W. Kantelhardt, T. Penzel, J. H. Peter, and K. Voigt, Phys. Rev. Lett. **85**, 3736 (2000).
[60] T. T. Laitio, H. V. Huikuri, E. S. H. Kentala, T. H. Makikallio, J. R. Jalonen, H. Helenius, K. Sariola-Heinonen, S. Yli-Mayry, and H. Scheinin, Anesthesiology **93**, 69 (2000).
[61] R. I. Kitney and O. Rompelman, *The Study of Heart-Rate Variability* (Oxford University Press, London, 1980).
[62] R. I. Kitney, D. Linkens, A. C. Selman, and A. A. McDonald, Automedica **4**, 141 (1982).
[63] L. S. Liebovitch, Adv. Chem. Ser. **235**, 357 (1994).
[64] J. Kurths, A. Voss, P. Saparin, A. Witt, H. J. Kleiner, and N. Wessel, Chaos **5**, 88 (1995).
[65] A. L. Goldberger, Lancet **347**, 1312 (1996).
[66] Y. Q. Chen, M. Z. Ding, and J. A. S. Kelso, Phys. Rev. Lett. **79**, 4501 (1997).
[67] B. J. West and L. Griffin, Fractals **6**, 101 (1998).
[68] S. B. Lowen, L. S. Liebovitch, and J. A. White, Phys. Rev. E **59**, 5970 (1999).
[69] S. Havlin, S. V. Buldyrev, A. Bunde, A. L. Goldberger, P. Ch. Ivanov, C.-K. Peng, and H. E. Stanley, Physica A **273**, 46 (1999).
[70] L. Griffin, D. J. West, and B. J. West, J. Biol. Phys. **26**, 185 (2000).
[71] H. E. Stanley, L. A. N. Amaral, P. Gopikrishnan, P. Ch. Ivanov, T. H. Keitt, and V. Plerou, Physica A **281**, 60 (2000).
[72] L. A. Protsmman, H. Meeuwsen, P. Hamilton, B. J. West, and J. Wilkerson, J. Sport Exerc. Psychol. **23**, S67 (2001).
[73] *Fractals and Disordered Systems*, 2nd ed., edited by A. Bunde and S. Havlin (Springer-Verlag, Berlin, 1996).
[74] H. Takayasu, *Fractals in the Physical Sciences* (Manchester University Press, Manchester, UK, 1997).
[75] S. Stoev, V. Pipiras, and M. S. Taqqu, Signal Process. **82**, 1873 (2002).
[76] H. E. Hurst, Trans. Am. Soc. Civ. Eng. **116**, 770 (1951).
[77] J. Feder, *Fractals* (Plenum, New York, 1988).
[78] T. Vicsek and A.-L. Barabási, J. Phys. A **24**, L845 (1991).
[79] A.-L. Barabasi, P. Szepfalusy, and T. Vicsek, Physica A **178**, 17 (1991).
[80] J. Nittmann, G. Daccord, and H. E. Stanley, Nature (London) **314**, 141 (1985).
[81] C. Meneveau and K. R. Sreenivasan, Phys. Rev. Lett. **59**, 1424 (1987).
[82] C. Li and C. Zheng, *Engineering in Medicine and Biology Society.*, Proceedings of the 15th Annual International Conference of the IEEE, edited by A. Y. J. Szeto, and R. M. Rangayyan(IEEE, New York,1993), Vol. 15, p. 330.
[83] O. Meste, H. Rix, P. Caminal, and N. V. Thakor, IEEE Trans. Biomed. Eng. **41**, 625 (1994).
[84] L. Senhadji, G. Carrault, J. J. Bellanger, and G. Passariello, IEEE Eng. Med. Biol. Mag. **14**, 167 (1995).
[85] M. Karrakchou, C. V. Lambrecht, and M. Kunt, IEEE Eng. Med. Biol. Mag. **14**, 179 (1995).
[86] N. V. Thakor, X. R. Guo, Y. C. Sun, and D. F. Hanley, IEEE Trans. Biomed. Eng. **40**, 1085 (1993).
[87] D. Morlet, J. P. Couderc, P. Touboul, and P. Rubel, Int. J. Biomed. Comput. **39**, 311 (1995).
[88] D. Morlet, F. Peyrin, P. Desseigne, P. Touboul, and P. Rubel, J. Electrocardiol. **26**, 311 (1993).
[89] L. Reinhardt, M. Mäkijärvi, T. Fetsch, J. Montonen, G. Sierra, A. Martínez-Rubio, T. Katila, M. Borggrefe, and G. Breithardt, J. Am. Coll. Cardiol. **27**, 53 (1996).
[90] M. Karrakchou and M. Kunt, Ann. Biomed. Eng. **23**, 562 (1995).
[91] P. Ch. Ivanov, M. G. Rosenblum, C.-K. Peng, J. Mietus, S. Havlin, H. E. Stanley, and A. L. Goldberger, Nature (London) **383**, 323 (1996).
[92] P. Ch. Ivanov, M. G. Rosenblum, C.-K. Peng, J. Mietus, S. Havlin, H. E. Stanley, and A. L. Goldberger, Physica A **249**, 587 (1998).
[93] J. F. Muzy, E. Bacry, and A. Arneodo, Phys. Rev. E **47**, 875 (1993).
[94] T. Vicsek, *Fractal Growth Phenomena*, 2nd ed. (World Scientific, Singapore, 1993).
[95] D. Panter, *Modulation, Noise and Spectral Analysis* (McGraw-Hill, New York, 1965).
[96] J. Theiler, S. Eubank, A. Longtin, B. Galdrikian, and D. J. Garmer, Physica D **58**, 77 (1992).
[97] J. W. Kantelhardt, Y. Ashkenazy, P. Ch. Ivanov, A. Bunde, S. Havlin, T. Penzel, J. H. Peter, and H. E. Stanley, Phys. Rev. E **65**, 051908 (2002).
[98] R. Karasik, N. Sapir, Y. Ashkenazy, P. Ch. Ivanov, I. Dvir, P. Lavie, and S. Havlin, Phys. Rev. E **66**, 062902 (2002).
[99] H. E. Stanley, L. A. N. Amaral, A. L. Goldberger, S. Havlin, P. Ch. Ivanov, and C.-K. Peng, Physica A **270**, 309 (1999).
[100] N. Tanaka, S. Sonoda, Y. Muraoka, Y. Tomita, and N. Chino, Jpn. J. Rehabil. Med. **33**, 549 (1996).
[101] U. Frisch, *Turbulence* (Cambridge University Press, Cambridge, UK, 1995).
[102] K. Hu, P. Ch. Ivanov, Z. Chen, M. F. Hilton, H. E. Stanley,

and S. A. Shea, Physica A **337**, 307 (2004).
[103] P. Ch. Ivanov, K. Hu, M. F. Hilton, S. A. Shea, and H. E. Stanley, Proc. Natl. Acad. Sci. U.S.A. **104**, 20702 (2007).
[104] R. Bartsch, M. Plotnik, J. W. Kantelhardt, S. Havlin, N. Giladi, and J. M. Hausdorff, Physica A **383**, 455 (2007).
[105] K. Ohgane and K. I. Ueda, Phys. Rev. E **77**, 051915 (2008).
[106] V. B. Kokshenev, Phys. Rev. Lett. **93**, 208101 (2004).
[107] P. Ch. Ivanov, L. A. N. Amaral, A. L. Goldberger, and H. E. Stanley, Europhys. Lett. **43**, 363 (1998).
[108] D. C. Lin and R. L. Hughson, Phys. Rev. Lett. **86**, 1650 (2001).
[109] P. V. E. McClintock and A. Stefanovska, Physica A **314**, 69 (2002).
[110] R. Yulmetyev, P. Hanggi, and F. Gafarov, Phys. Rev. E **65**, 046107 (2002).